Poster2-06 **A FIRST LOOK AT THE ATD DATA CORRECTIONS**

Igor R. Ivić* and David Schvartzman

Cooperative Institute for Mesoscale Meteorological Studies, University of Oklahoma, and
NOAA/OAR/National Severe Storms Laboratory, Norman, Oklahoma

1. INTRODUCTION

The Advanced Technology Demonstrator (ATD) is an S-band planar polarimetric phased array radar (PPAR) that is funded through a joint collaboration of the National Oceanic and Atmospheric Administration (NOAA) and the Federal Aviation Administration (FAA). It is being developed by the National Severe Storms Laboratory (NSSL), MIT Lincoln Laboratory, and General Dynamics Mission Systems (Stailey and Hondl 2016). The main purpose of this system is to serve as testbed for evaluating the suitability of phased array radar (PAR) technology for weather observations (Zrnić et al., 2007).

One of the major obstacles to the use of PPAR technology for weather surveillance is the calibration needed to achieve measurements comparable to those of the systems using parabolic-reflector antennas (Zrnić et al 2012). This is due to the existence of significant cross-polar antenna patterns, as well as the scan-dependent measurement biases, inherent to PPAR (Ivić 2018, Fulton et al. 2018). The former induces cross coupling between returns from the horizontally and vertically oriented fields resulting in the biases of polarimetric variable estimates. Furthermore, the inductive and capacitive coupling in hardware may exacerbate the cross-coupling effects.

Pulse-to-pulse phase coding in either the horizontal or vertical ports of the transmission elements has been proposed to mitigate the cross-coupling effects (Zrnić et al., 2014, Ivić 2017a, Ivić 2017b, Ivić 2018a). This approach, however, does not address the scan-dependent system biases in PPAR estimates. These are caused by the horizontal (H) and vertical (V) copolar antenna patterns which vary with beamsteering direction. The effects of these variations must be addressed via corrections using appropriate values at each boresight location. If the cross-coupling effects are sufficiently suppressed with phase coding and given sufficiently narrow antenna main beam, the corrections can be conducted using only the beam peak values of the copolar patterns (Ivić 2018b). But, the cross coupling mitigation from pulse-to-pulse phase coding is inversely proportional to the cross-polar pattern levels. Thus, at boresight locations where the cross-polar pattern levels are too high the correction using the beam peak values of both the copolar and cross-polar patterns needs to be conducted. Furthermore, the effects of active electronic components in transmit and receive paths in PAR systems can result in significant differences between transmit and receive patterns. For these reasons it is important to characterize the peaks of both transmit as well as receive copolar and cross-polar antenna patterns (Ivić 2019).

In this work, a first look at the beam-peak-based corrections using data from the ATD system is presented. The paper is structured as follows. In section 2, an overview of calibration concepts and the calibration infrastructure are presented, Section 3 illustrates the correction methods described on real data collected with the ATD and provides a quantitative comparison between non-corrected and corrected data. The summary is given in section 4.

2. POLARIMETRIC CORRECTION

The ATD antenna is designed by MIT Lincoln Laboratory (Conway et al., 2013) and uses differential-fed single radiating elements (Bhardwaj and Rahmat-Samii, 2014). The antenna is composed of 76 panels arranged as shown in Fig. 1. Each panel consists of an 8×8 set of radiating patch-antenna elements with dual linear polarization (H and V), for a total of 4864 elements. This arrangement of antenna elements, spaced by λ/2, results in a ~4×4 m aperture which produces a

* *Corresponding author address:* Igor R. Ivić, 120 David L. Boren Blvd, Room 4415, Norman, OK, 73072; e-mail: igor.ivic@noaa.gov.

beam that is ~1.6° wide at broadside. On receive, the antenna is partitioned into overlapped subarrays (consisting of 8 panels each) to produce lower sidelobes and suppress grating lobes outside of the main beam of the subarray pattern (Herd et al, 2005). The operating frequency band of the antenna is 2.7-3.1 GHz.

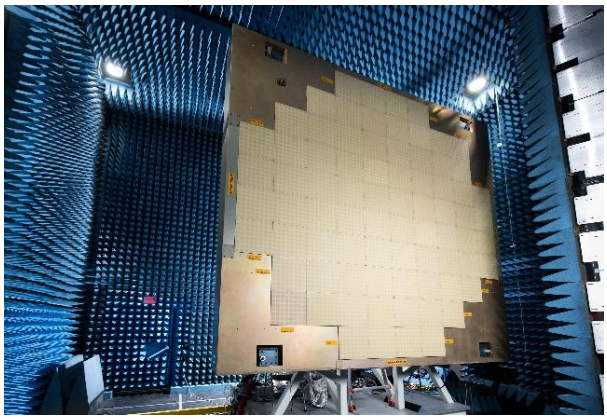

Fig. 1. ATD antenna in the anechoic chamber at MIT-Lincoln Laboratories. Courtesy of Alexander Morris from MIT-Lincoln Laboratories.

The calibration infrastructure for the ATD includes a 45.7 m tall far-field calibration tower, located 428 m north of the ATD site. Atop the tower, an S-band standard gain horn is mounted at the height of ~45 m. It is attached to a motorized platform that allows it to rotate about its axis and set the horn polarization in horizontal, vertical or any other desired position. This infrastructure is currently being developed and integrated into the ATD system and it will be used to obtain accurate beam-peak measurements of the fielded array. Accurate beam peak measurements of copolar patterns can be used to correct the antenna induced copolar biases in differential reflectivity (Z_{DR}) and phase (ϕ_{DP}) estimates as well as to correct reflectivity (Z) (Doviak and Zrnić, 1993) as the beam is steered away from broadside (assuming the known system calibration constant for Z at broadside). Further, the described infrastructure will be used to measure the peaks of cross-polar ATD antenna patterns. In combination with copolar peaks, these may be used to create the full correction matrices which account for the copolar biases and mitigate the effects of cross coupling at the same time. These matrices may be used for correction at beamsteering locations where the cross-polar patterns are high and the cross coupling suppression via pulse-to-pulse phase coding is insufficient.

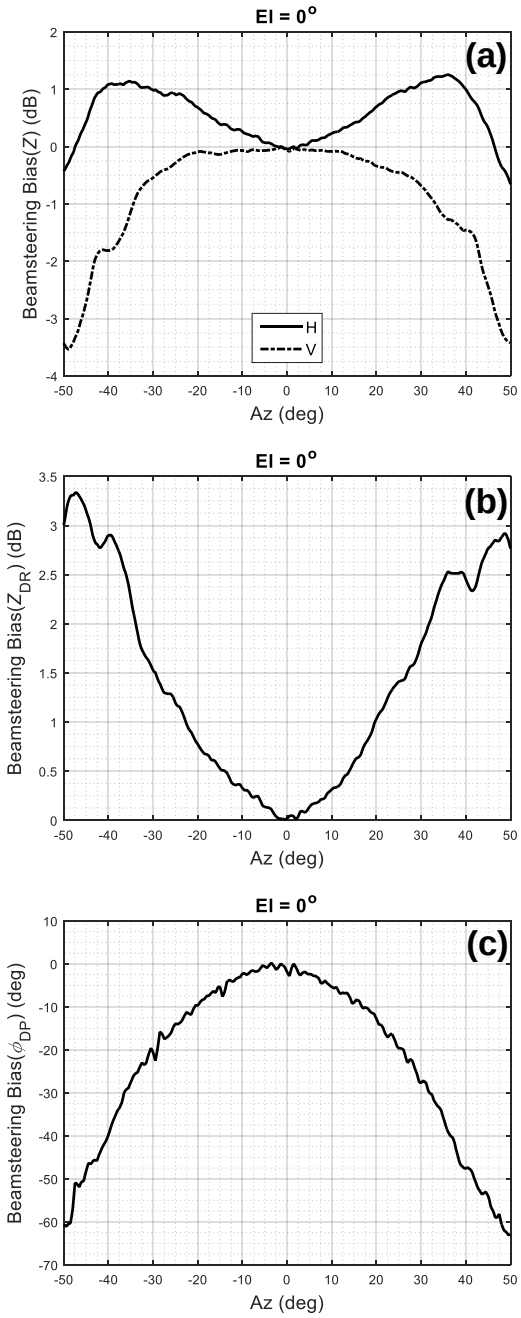

Fig. 2. Near-field measured copolar beamsteering biases. (a) Reflectivity in H and V. (b) Differential reflectivity (c). Differential phase.

Prior to installation in Norman OK, the ATD antenna transmit and receive copolar as well as cross-polar patterns were measured in the near-field chamber at the MIT-Lincoln Laboratory facilities during March-April 2018 (Conway et al., 2018). The patterns were collected for a total of 2859 electronic beamsteering positions. By extracting the copolar beam peaks along the horizontal cardinal plane, the copolar biases for Z,

Z_{DR} and ϕ_{DP} are computed and shown in Fig. 2. Note that the biases are scaled to broadside.

Given that the data from the ATD calibration infrastructure is not yet available, the near-field measurements (shown in Fig. 2) are used herein for initial correction assessment. These measurements may not represent the current state of the array with utmost accuracy since they were obtained about a year prior to the collection of data analyzed here. Further, the ATD antenna was disassembled and reassembled for transportation and installation in Norman, OK. Nevertheless, comparing power outputs of each element during the near-field experiment (April 2018) to those with the ATD system fielded in Norman (May 2019) shows little to no increase in failed elements. Specifically, this comparison indicated 11 and 6 additional transmit elements failures on the horizontal and vertical polarizations, respectively. Thus, given the small change in the state of failed elements in the array, and assuming that the radar is sufficiently stable with time and temperature, the near-field measurements are used herein to correct for the copolar biases.

In the next section, we use the near-field measurements to derive copolar bias corrections, and we conduct a preliminary assessment of the correction performance using ATD data.

3. CORRECTION ASSESSMENT

Data, used in the analysis herein, were collected during the May 1st, 2019 severe weather event using pulse-to-pulse phase coding. For this data collection, the antenna was perpendicular to the ground and the beam was electronically steered ±45° in azimuth and elevation at both the 0.5° and 0.9° angles. Because the beam was steered close to the horizontal principal plane, it is assumed that the effects of cross coupling are sufficiently suppressed via phase coding. Pulse compression with a pulse length of 38 µs was used to increase sensitivity. It was followed by a 1.8 µs fill pulse to collect data at close range blanked by the previous 38 µs long pulse.

During the collection, the array was mechanically rotated in azimuth by ~7° at 19:58:45 UTC, changing the boresight direction from 192° to 185° azimuth with respect to north. The scans before and after the rotation (herein Scan 1 and Scan 2, respectively) were processed with and without copolar bias corrections. The overlapping parts of the scans are used to assess the difference in estimated polarimetric variables from collocated volumes illuminated using distinct electronic steering angles (herein referred to as self-consistency). The differences are analyzed when no corrections are applied for the effects of beamsteering and after applying the copolar polarimetric corrections derived from the near-field measurements.

Radar variable estimates of Z, Z_{DR}, ϕ_{DP}, and $|\rho_{hv}(0)|$ (the copolar correlation coefficient) are shown in the columns of Fig. 3. From top to bottom, the rows of Fig. 3 show: uncorrected ATD estimates from Scan 1, corrected ATD estimates from Scan 1, uncorrected ATD estimates from Scan 2, corrected ATD estimates from Scan 2, and data from the closely located Twin Lakes (KTLX) operational WSR-88D radar for reference. In addition, the ATD estimates of Z, Z_{DR}, and ϕ_{DP} are adjusted by corresponding constant values (i.e., system calibration constants) at all beamsteering locations to visually resemble the KTLX data. Note that the copolar correlation coefficient estimates are inherently impervious to the variations in copolar biases shown in Fig. 2 (a) and therefore do not require copolar corrections. Also, because the scans are conducted close to H principal plane it is assumed that the cross-coupling effects are non-significant.

ATD data presented in rows 1 and 3 of Fig. 3 are processed with no corrections applied to account for beamsteering variations. Visual comparison between the ATD and KTLX fields of Z and $|\rho_{hv}(0)|$ exhibits good similarity despite the reduced SNR visible in the ATD data. Visual comparison between the Z_{DR} and ϕ_{DP} fields indicates a system induced Z_{DR} increase and ϕ_{DP} decrease in the ATD fields as the beam is steered away from the vertical principal plane. These are the same trends as indicated in Fig. 2. Next, using near-field measurements to correct the Z, Z_{DR} and ϕ_{DP} beamsteering biases results in the fields presented in rows 2 and 4 on Fig. 3. Visual inspection reveals that the Z_{DR} and ϕ_{DP} fields

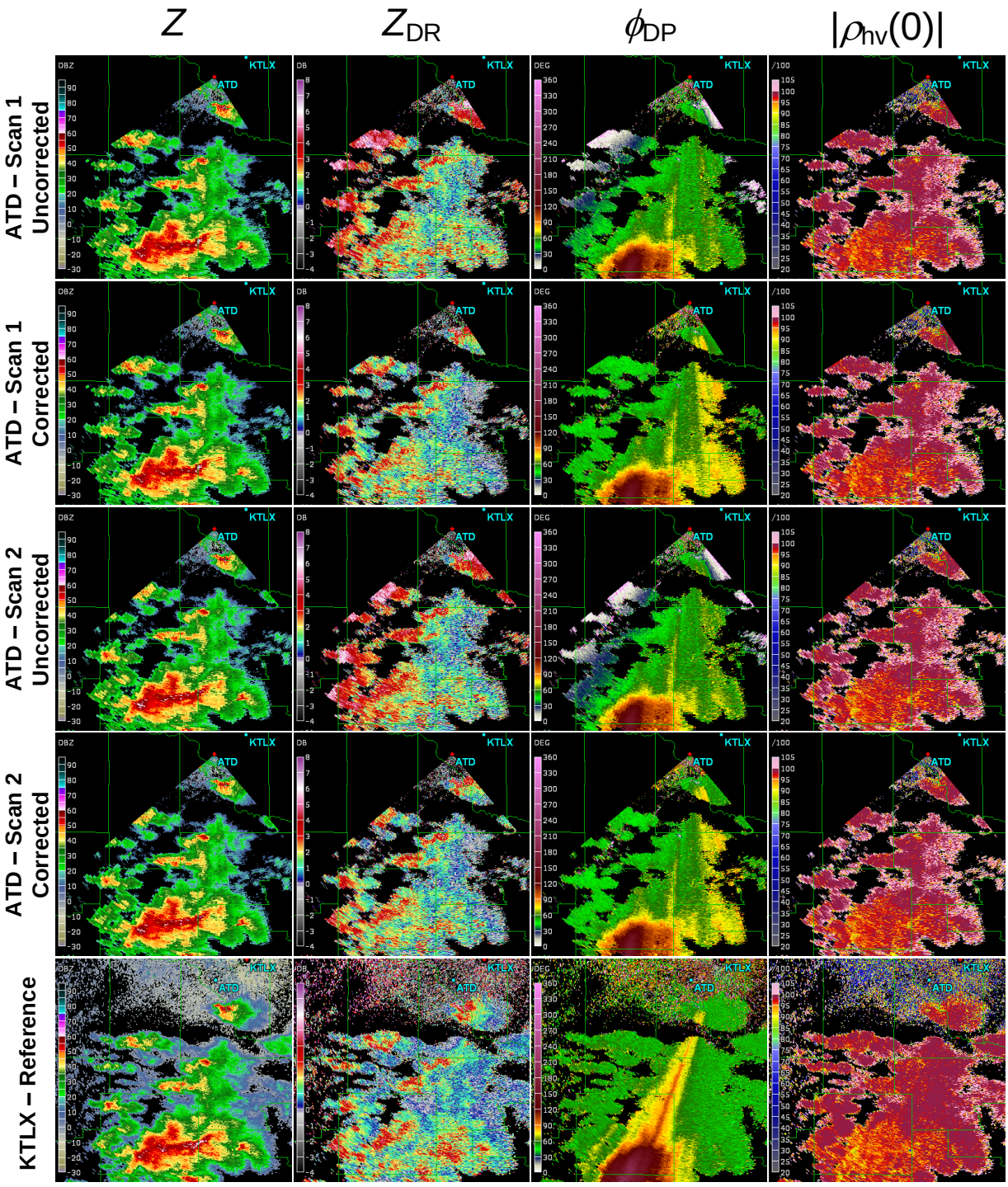

Fig. 3. Data collected on 01 May 2019 in Norman, OK with the ATD system. The array boresight on ATD Scan 1 is at 192° azimuth (rows 1 and 2) and for ATD Scan 2 at 185° azimuth (rows 3 and 4). ATD Scan 1 was collected at 195835 UTC and ATD Scan 2 was collected at 195907 UTC. For both scans, the antenna was perpendicular to the ground and the beam was electronically steered ±45 in azimuth and 0.5° in elevation. For reference, data collected with the closely located operational KTLX WSR-88D are shown on the bottom row.

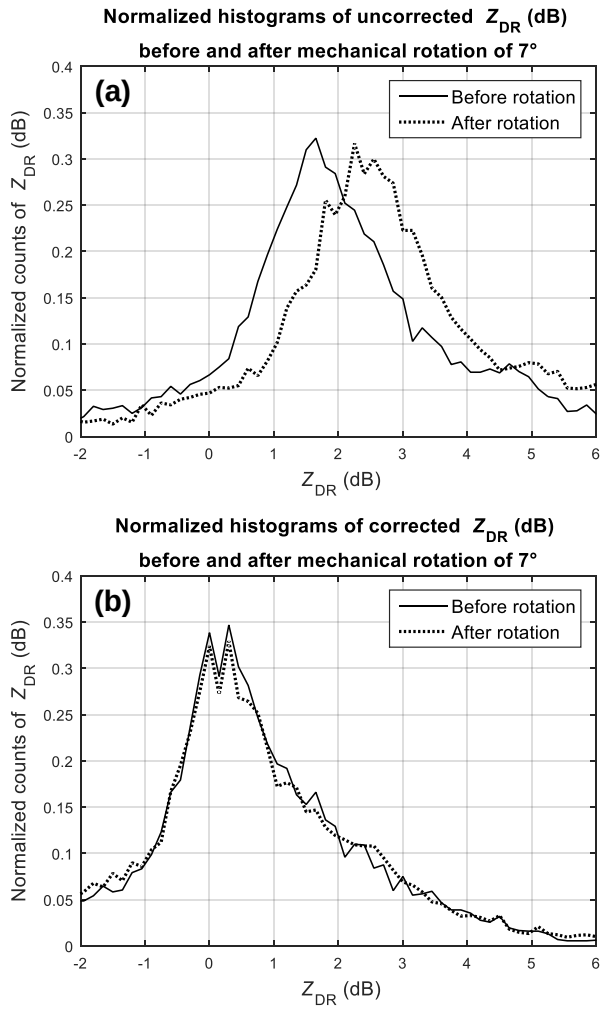

Fig. 4. Normalized histograms of Z_{DR} estimates (a) no beamsteering corrections, (b) with beamsteering corrections.

exhibit improved similarity to those of KTLX, indicating that corrections based on near-field measurements are reducing beamsteering biases away from 0° azimuth. It is promising that the near-field data captured the trends in the beamsteering biases in the weather data collected more than a year later.

To quantify the self-consistency of the ATD estimates, data in the intersection of Scan 1 and Scan 2 are computed before and after the mechanical rotation of the antenna. Given that beamsteering biases are low close to broadside, a 20° sector near the edge of the intersection is extracted for analysis (210° to 230° absolute azimuth). Fig. 4 (a) shows normalized histograms of uncorrected Z_{DR} estimates from this sector, before and after the rotation. Comparing these histograms reveals significant changes in the distribution of uncorrected Z_{DR} estimates when collocated volumes are illuminated using different electronic steering angles. Similarly, Fig. 4 (b) shows normalized histograms of corrected Z_{DR} estimates before and after the rotation. These are in very good agreement, indicating that collocated volumes illuminated using different electronic steering angles result in similar differential reflectivity estimates. Similar results were obtained for ϕ_{DP} estimates (not shown here).

Next, we estimated Z, Z_{DR}, and ϕ_{DP} differences between Scans 1 and 2 at each data location and averaged them in range before and after the corrections were applied. Assuming no appreciable changes in weather between Scans 1 and 2, the differences between uncorrected estimates should produce the difference between the beamsteering biases. This is because the subtraction of uncorrected estimates cancels the weather contributions (up to the statistical uncertainty) leaving the difference between system induced biases at the two electronic steering angles used to illuminate the particular area of space. Further, the ensemble average of every difference estimate at each range location along a given radial is expected to be the same so the range average is applied to reduce the standard deviation of estimates. The difference between the corrected estimates, on the other hand, should exhibit zero difference on the average. The results of this exercise are presented in Fig. 5 along with bias differences computed from the near-field measurements. In case of reflectivity bias differences, the estimates from Scans 1 and 2 exhibit considerably high variances compared to ~1 dB change in steering loss indicated in Fig. 2 (a) (note that Z is estimated from returns in the H channel), but appear to generally follow the curves computed from the near-field measurements. Estimated Z_{DR}, and ϕ_{DP} bias differences exhibit visible agreement with the near-field results. Accordingly, the difference estimates from the corrected data indicate improvement in the self-consistency of Z_{DR}, and ϕ_{DP} estimates from the two scans (i.e., the full lines appear to fluctuate around zero bias). This is corroborated by the mean values of the corrected differences across all azimuths which are -0.0024 dB, -0.015 dB, and -0.15° for Z, Z_{DR}, and ϕ_{DP} differences, respectively.

4. SUMMARY

Calibration of PPAR for weather observations requires corrections to account for transmit and receive pattern variations as H and V beams are electronically steered in various directions. Given the sufficient suppression of cross–coupling effects (e.g., via pulse-to-pulse phase coding), this can be achieved using knowledge of copolar beam peaks at boresight locations of interest. If the cross-coupling effects cannot be adequately mitigated, a full correction using both copolar and cross-polar beam peaks may be possible. This necessitates the need for the measurements of the copolar and cross-polar pattern peaks on the ATD.

In this work, the concept is demonstrated using real weather data collected with the ATD radar system and applying corrections derived from near-field measurements. Preliminary results presented here show that the estimated polarimetric variables computed from collocated volumes illuminated using distinct electronic steering angles exhibit differences that generally agree with the differences computed from near-field measurements. Consequently, application of the polarimetric corrections (based on the results of near-field measurements) significantly reduced the difference among the differential reflectivity and differential phase estimates associated with collocated volumes illuminated using distinct electronic steering angles.

The demonstrated corrections show promise, even though they are based on previous near-field measurements. A calibration infrastructure is currently being integrated to the ATD system to obtain actual far-field measurements of the array. The preliminary results presented in this paper, indicate that the accurate far-field measurements can be used to correct the system induced copolar biases.

ACKNOWLEDGMENT

The authors would like to acknowledge the contributions of numerous engineers, students, scientists, and administrators who have supported these developments over the last decade.

This conference paper was prepared with funding provided by NOAA/Office of Oceanic and Atmospheric Research under NOAA-University of Oklahoma Cooperative Agreement #*NA16OAR4320115*, U.S. Department of Commerce. The statements, findings, conclusions, and recommendations are those of the authors and do not necessarily reflect the views of NOAA or the U.S. Department of Commerce.

REFERENCES

Bhardwaj, S., and Y. Rahmat-Samii, 2014: Revisiting the generation of cross-polarization in rectangular patch antennas: A near-field approach. *IEEE Antennas Propag. Mag.*, **56**, 14–38, doi:https://doi.org/10.1109/MAP.2014.6821758.

Conway, D., J. Herd, M. Fosberry, M. Harger, C. Weigand, M. Yeary, and K. Hondl, 2013: On the development of a tileable LRU for the nextgen surveillance and weather radar capability program. *2013 IEEE International Symposium on Phased Array Systems and Technology*, IEEE, 490–493, doi:https://doi.org/10.1109/ARRAY.2013.6731877.

Conway, M. D., D. Du Russel , A. Morris, and C. Parry, 2018: Multifunction phased array radar advanced technology demonstrator nearfield test results. *Proc. of the IEEE,* doi: https://doi.org/10.1109/RADAR.2018.8378771

Doviak, R. J., and D. S. Zrnić, 1993: *Doppler Radar and Weather Observations*. Academic Press, 562 pp.

Fulton, C., J. Salazar, D. Zrnić, D. Mirković, I. Ivić, and D. Doviak, 2018: Polarimetric Phased Array Calibration for Large-Scale Multi-Mission Radar Applications, *IEEE Radar Conference (RadarConf18)* doi: https://doi.org/10.1109/RADAR.2018.8378746

Herd, J. S., S. M. Duffy, and H. Steyskal, 2005: Design considerations and results for an overlapped subarray radar antenna. Preprints, *IEEE Aerospace Conf.*, Big Sky, MT, doi: http://dx.doi.org/10.1109/AERO.2005.1559399

Ivić, I. R., and R. J. Doviak, 2016: Evaluation of phase coding to mitigate differential reflectivity bias in polarimetric PAR. *IEEE Trans. Geosci. Remote Sens.*, **54**, 431–451, doi:https://doi.org/10.1109/TGRS.2015.2459047

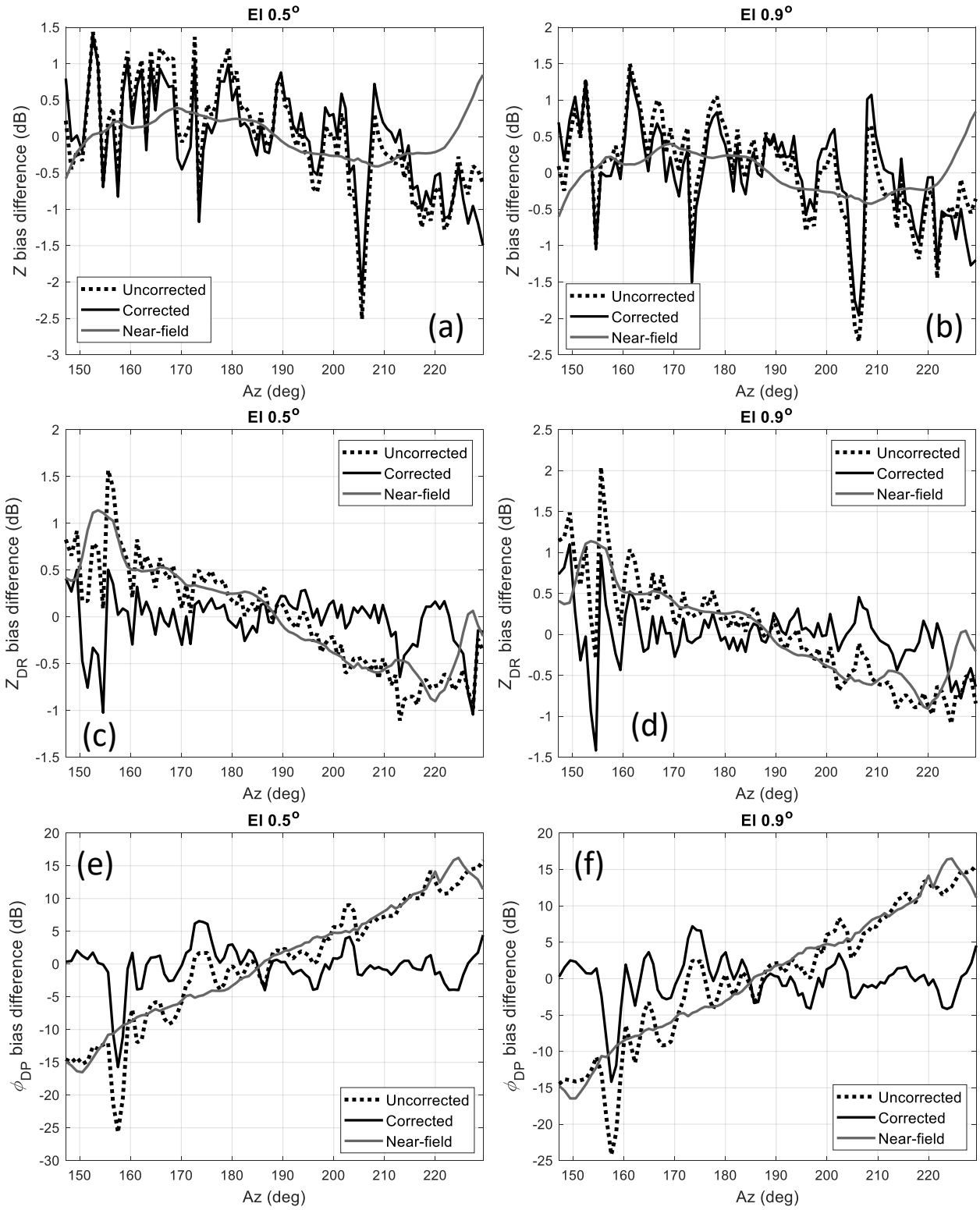

Fig. 5. Z, Z_{DR}, and ϕ_{DP} bias differences computed from uncorrected (dotted lines) and corrected (full lines) Scan 1 and 2 estimates as well as from the near-field measurements (full grey lines). The bias differences are produced from scans at 0.5° (left column) and 0.9° (right column) elevations.

Ivić, I. R., 2017a: Phase Code to Mitigate the Copolar Correlation Coefficient Bias in PPAR Weather Radar. *IEEE Trans. Geosci. Remote Sensing*, *GE-55(**4**)*, 2144-2166, doi: https://doi.org/10.1109/TGRS.2016.2637720

Ivić, I. R., 2017b: An experimental evaluation of phase coding to mitigate the cross-coupling biases in PPAR. *Preprints 38th International Conference on Radar Meteorology,* Chicago, IL.

Ivić, I. R., 2018: Options for Polarimetric Variable Measurements on the MPAR Advanced Technology Demonstrator, *IEEE Radar Conference (RadarConf18)*, doi: https://doi.org/10.1109/RADAR.2018.8378544

Ivić, I. R., 2018a: Effects of Phase Coding on Doppler Spectra in PPAR Weather Radar. *IEEE Trans. Geosci. Remote Sensing*, *GE-56(**4**)*, 2043 – 2065, doi: https://doi.org/10.1109/TGRS.2017.2772962

Ivić, I.R., 2018b: On the Use of Horn Antenna to Calibrate the MPAR Advanced Technology Demonstrator. *10th European Conference on Radar in Meteorology and Hydrology*, Wageningen, Netherlands.

Ivić, I. R., 2019: Facets of Planar Polarimetric Phased Array Radar Use for Weather Observations. *AMS 99th Annual Meeting,* Phoenix, AZ.

Stailey, J. E., and K. D. Hondl, 2016: Multifunction phased array radar for aircraft and weather surveillance. *Proc. IEEE*, **104**, 649–659, doi: https://doi.org/10.1109/JPROC.2015.2491179.

Zrnić, D. S., and Coauthors, 2007: Agile-beam phased array radar for weather observations. *Bull. Amer. Meteor. Soc.*, **88**, 1753–1766, https://doi.org/10.1175/BAMS-88-11-1753.

Zrnić, D. S., V. M. Melnikov, and R. J. Doviak, 2012: Issues and challenges for polarimetric measurement of weather with an agile beam phased array radar. NOAA/NSSL Rep., 119 pp. [Available online:http://www.nssl.noaa.gov/publications/mpar_reports/]

Zrnić, D.S., R.J. Doviak, V.M. Melnikov, and I.R. Ivić, 2014: Signal Design to Suppress Coupling in the Polarimetric Phased Array Radar. *J. Atmos. Oceanic Technol.,* **31**, 1063–1077, https://doi.org/10.1175/JTECH-D-13-00037.1.